Perpendicular magnetic anisotropy at the interface between ultrathin Fe film and MgO studied by angular-dependent x-ray magnetic circular dichroism

J. Okabayashi, J. W. Koo, H. Sukegawa, S. Mitani, Y. Takagi, and T. Yokoyama

Citation: Applied Physics Letters **105**, 122408 (2014); doi: 10.1063/1.4896290
View online: http://dx.doi.org/10.1063/1.4896290
View Table of Contents: http://scitation.aip.org/content/aip/journal/apl/105/12?ver=pdfcov
Published by the AIP Publishing

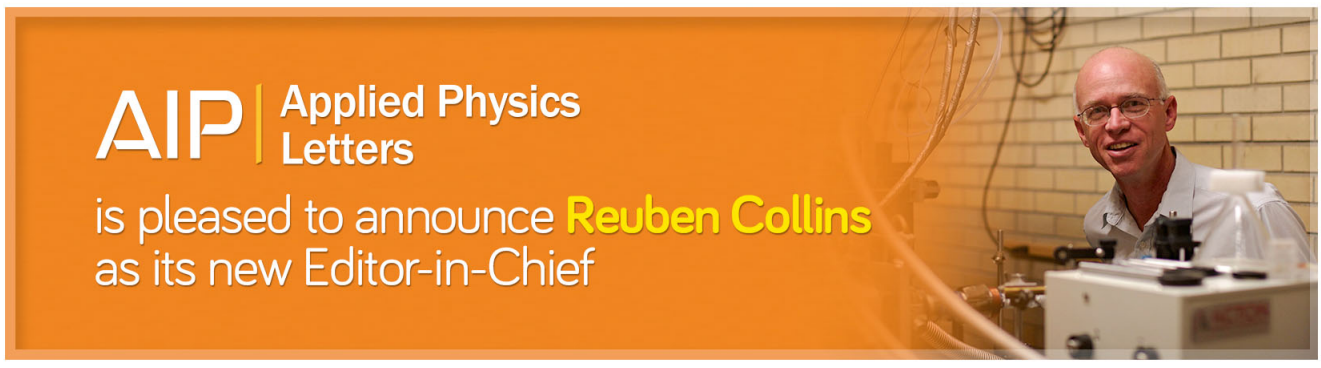

Perpendicular magnetic anisotropy at the interface between ultrathin Fe film and MgO studied by angular-dependent x-ray magnetic circular dichroism

J. Okabayashi,[1] J. W. Koo,[2,3] H. Sukegawa,[2] S. Mitani,[2,3] Y. Takagi,[4] and T. Yokoyama[4]
[1]*Research Center for Spectrochemistry, The University of Tokyo, Bunkyo-ku, Tokyo 113-0033, Japan*
[2]*National Institute for Materials Science (NIMS), Tsukuba 305-0047, Japan*
[3]*Graduate School of Pure and Applied Sciences, University of Tsukuba, Tsukuba 305-8577, Japan*
[4]*Institute of Molecular Science, Okazaki, Aichi 444-8585, Japan*

(Received 20 July 2014; accepted 4 September 2014; published online 26 September 2014)

Interface perpendicular magnetic anisotropy (PMA) in ultrathin Fe/MgO (001) has been investigated using angular-dependent x-ray magnetic circular dichroism (XMCD). We found that anisotropic orbital magnetic moments deduced from the analysis of XMCD contribute to the large PMA energies, whose values depend on the annealing temperature. The large PMA energies determined from magnetization measurements are related to those estimated from the XMCD and the anisotropic orbital magnetic moments through the spin-orbit interaction. The enhancement of anisotropic orbital magnetic moments can be explained mainly by the hybridization between the Fe $3d_z^2$ and O $2p_z$ states.
 [http://dx.doi.org/10.1063/1.4896290]

Perpendicular magnetic anisotropy (PMA) is an important topic in spintronics research because of the advantages of thermal stability enhancement and the low current magnetization switching, which allow the development of low-power-consumption operation in spintronics devices such as magnetoresistive random access memories (MRAMs). Since the discovery of large tunnel magnetoresistance in single-crystal MgO-based magnetic tunnel junctions,[1] the interfaces between MgO and magnetic layers have been investigated thoroughly. Recently, large PMA energies of 0.21 MJ/m^3 have been developed by utilizing the interfaces between MgO and CoFeB transition metal alloys[2] that are comparable to the PMA in Co/Pt multilayers.[3] This finding has initiated the development of high-performance MRAM using the interface PMA. For a fundamental understanding of the induction of PMA at the interface between a ferromagnetic layer and a MgO barrier layer, the electronic and magnetic structure of the interface between an ultrathin Fe layer and MgO must be clarified explicitly from the viewpoint of band dispersions.[4,5] This would also provide an explanation for the origin of PMA at the interface between FeCo-based alloys and MgO.[6] Density functional theory (DFT) calculations revealed that a larger PMA appears at the interface between Fe and MgO than that of Co/MgO interfaces because of the difference in 3*d* orbital occupancies.[7] It has also been reported that the oxygen stoichiometry at the interface between Fe and MgO strongly depends on the PMA energies; namely, the over- and under-oxidization at the interface reduces the PMA. Experimentally, Koo *et al.*[8] found that the PMA energies depend on the interface conditions and are controllable by the post-annealing process at the ultrathin 0.7-nm-thick Fe/MgO interface. There are several experimental reports about the amplitude of PMA energies,[8–10] and the maximum interfacial PMA is reported as 2.0 mJ/m^2.[8] The values of PMA are of the same order of magnitude as those estimated by theoretical calculations. In order to investigate the PMA energy (K_{eff} [unit in J/m^3]), it is necessary to evaluate microscopically the orbital magnetic moments along parallel and perpendicular directions to the surface. Spin-orbit coupling is an essential factor concerning the origin of the interface PMA. The model proposed by Bruno for the quantitative estimation of the PMA energies through the second-order perturbation for the spin-orbit interaction is related to the anisotropic orbital magnetic moments in parallel and perpendicular to the surface.[11,12] Detailed investigations of the interface PMA in Fe/MgO systems from the viewpoint of the orbital magnetic moments are required for the understanding of the fundamental physics of the interface PMA. Furthermore, the interpretation of recent extensive investigations of electric-field-dependent modulations in PMA theoretically[13–16] and experimentally[17] necessitates an explicit clarification of the origin of PMA in Fe/MgO interfaces.

In order to investigate the orbital magnetic moments, x-ray magnetic circular dichroism (XMCD), associated with spectral analysis using magneto-optical sum rules,[18–20] constitutes a powerful technique. XMCD studies for Fe/MgO systems have been performed in the past.[21,22] However, the origin of the large PMA in Fe/MgO has not yet been established because of the necessity of a large saturation magnetic field along the hard magnetization axis. Angular-dependent XMCD enables us to deduce the anisotropic orbital magnetic moments and investigate the large PMA at the Fe/MgO interface. In particular, Fe/MgO systems with different annealing conditions, which give rise to different PMA values, can provide the interpretation of the relationship between anisotropic orbital magnetic moments and PMA energies.

In this paper, we report the anisotropic interface orbital magnetic moments of ultrathin Fe facing a MgO layer by using angular-dependent XMCD. Additionally, we discuss the PMA energies deduced from the orbital magnetic moments and the interfacial electronic and magnetic structures from the viewpoint of orbital magnetic moments.

Samples were grown by using an ultra-high vacuum electron-beam evaporation on MgO (001) substrates. The sample structures are shown in Fig. 1(a). After cleaning the MgO (001) substrate at 1000 °C, a 5-nm-thick MgO layer was deposited on the substrate at 450 °C and a 30-nm-thick

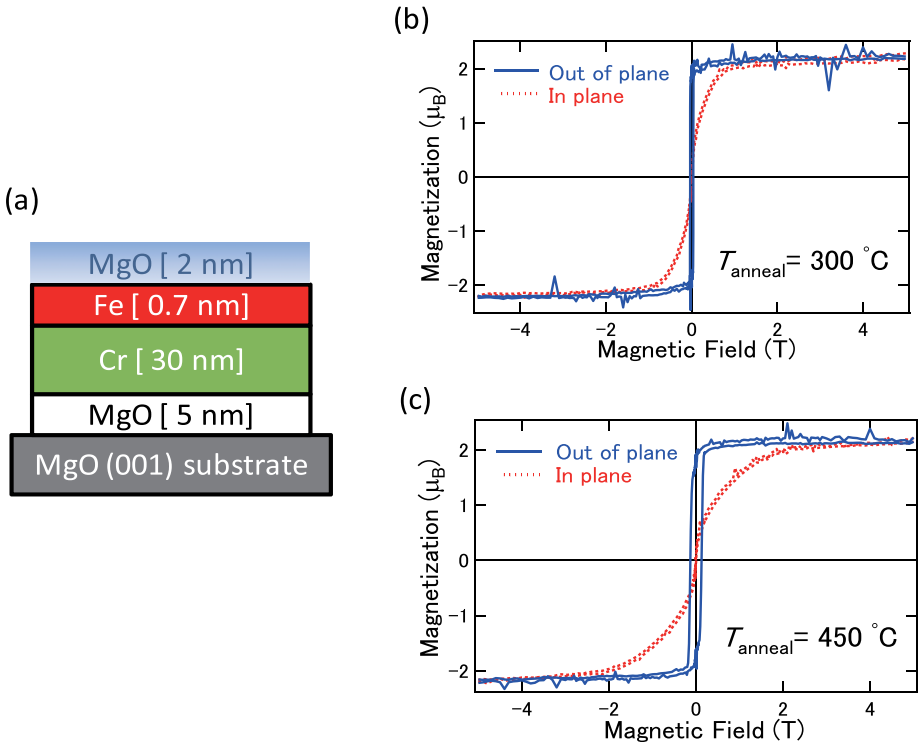

FIG. 1. (a) Sample structure with the film thicknesses. (b) and (c) The *M-H* loops measured by SQUID-VSM after the post-annealing at (b) 300 °C and (c) 450 °C.

Cr buffer layer at 150 °C. Subsequently, the annealing process was performed at 800 °C in order to prepare the flat surface. A 0.7-nm-thick Fe layer, which corresponds to 5 monolayers (MLs), was deposited on the Cr buffer layer at 150 °C and a MgO layer was also grown on the Fe layer at 150 °C. After the deposition of the MgO capping layer, two kinds of samples prepared with the above conditions were post-annealed separately at 300 or 450 °C in order to enhance the PMA. Magnetization curves were measured as functions of the magnetic fields (*M-H*) using superconducting quantum interference devices with a vibrating sample magnetometer (SQUID-VSM) at room temperature. Details of the surface and interface conditions and the fabrication procedures are reported in Ref. 8.

X-ray absorption spectroscopy (XAS) and XMCD measurements for Fe *L*-edges were performed at the UVSOR BL-4B beamline, Institute of Molecular Science, Japan, under conditions of 5 K.[23] Magnetic fields (H_{ext}) of ±5 T were applied using a superconducting magnet along the incident polarized soft X-rays in order to sufficiently saturate the magnetization along the direction of the magnetically hard axis. The total electron yield mode was adopted by detecting the drain currents from the samples. We changed the magnetic field directions in order to obtain right- and left-hand-side polarized X-rays while fixing the polarization direction of the incident X-ray. Angular-dependent XMCD was performed by rotating the angle between the incident beam and the direction of the sample's surface normal from the surface normal to 60°; these geometries are defined as normal incidence (NI) and grazing incidence (GI), respectively. In the case of the NI configuration, where both the photon helicity and the magnetic field directions are normal to the surface, the X-ray absorption processes involve the normal direction components of the orbital angular momentum ($m_{orb}^{\perp}$). The GI configuration mainly allows the detection of only the in-plane orbital momentum components ($m_{orb}^{\parallel}$).

Figures 1(b) and 1(c) show the *M-H* curves measured by SQUID-VSM at room temperature with respect to the applied magnetic field with the directions parallel and perpendicular to the sample surface. After post-annealing at 300 or 450 °C, distinct PMA characteristics were observed with different anisotropic fields in both cases. The saturation magnetization ($\mu_0 M_s$) of 2 T, which corresponds to 2.2 μ_B for Fe atom is consistent with the value of bulk Fe. In order to saturate the magnetization along the hard axis, magnetic fields of ±2 T are necessary. A coercive field of 0.13 T was observed in the 450 °C annealing case. Since the area of the *M-H* curves surrounded between the out-of-plane and in-plane directions corresponds to the PMA energy, the PMA in the case of the 450 °C annealing was estimated to be larger than that at 300 °C. For the annealing temperatures of 300 and 450 °C, the crystalline magnetic anisotropy energies (K_{eff} [J/m^3]) were estimated to be 0.38 and 1.4 MJ/m^3, respectively. Interface anisotropy energies (K_i [J/m^2]) are related by the following relationship: $K_{eff} = K_v + K_i/t$, where K_v is the volume anisotropy corresponding to the diamagnetic contribution ($-(\mu_0/2)M_s^2$) and t [nm] denotes the layer thickness. Using this relation, the values of K_i were deduced as 1.15 and 2.1 mJ/m^2 for 0.7-nm-thick Fe/MgO structures annealed at 300 and 450 °C, respectively. These differences correspond to the interface conditions. The annealing at 450 °C is the optimum condition to obtain large PMA energy.[8] It must be noted that, after the annealing at 500 °C, the easy magnetization axis was turned out to the direction parallel to the film plane, which might result from the intermixing at the other interface between Fe and Cr layers.

Figure 2(a) shows the XAS of a 0.7-nm-thick Fe/MgO interface after the annealing at 450 °C. The XMCD taken at the NI and GI geometries and the integrals of the Fe $L_{2,3}$

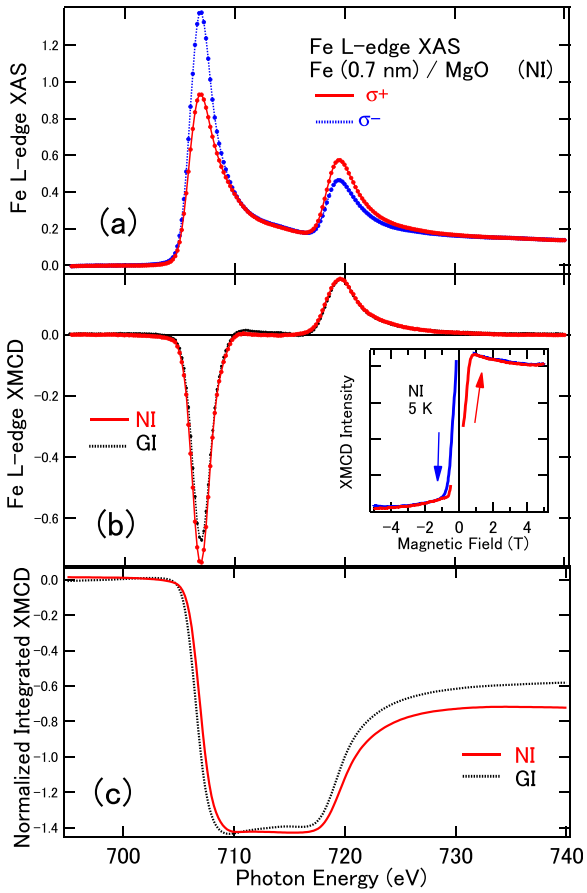

FIG. 2. (a) X-ray absorption spectra of 0.7-nm-thick Fe/MgO structures for an annealing temperature of 450 °C, measured in the NI geometry. (b) XMCD spectra of the NI and GI setups. (c) Integrated XMCD spectra of the NI and GI setups. Inset of (b) shows the magnetic field dependence at L_3 peak in the NI geometry.

absorption edges XMCD spectra are also shown in Figs. 2(b) and 2(c). Distinct metallic peaks are evident in the XAS of the Fe $L_{2,3}$ edges, which indicates that no atomically mixed layer formation with oxygen atoms occurred at the interface, even after the 450 °C annealing process. There are clear differences in the XAS spectra between right- and left-hand-side polarized X-rays and they reveal the XMCD signals. Since the XAS spectra obtained from the NI and GI setups were identical, only the XAS spectra in the NI configuration are shown. In Fig. 2(b), the XMCD spectra in the NI and GI setups display a distinct difference in the intensity between the L_3 edges while the L_2 edges show almost similar intensity. The measured XMCD signal for the Fe L_3 edge from the NI geometry was larger than that from the GI geometry, which suggests that the large orbital magnetic moments are induced when the H_{ext} is perpendicular to the film plane. The magneto-optical sum rule indicates that the integrated areas of both negative L_3 and positive L_2 peaks are proportional to the orbital magnetic moments.[18] The residuals of the integrals of both L_3 and L_2 edges in the XMCD spectra are larger in the NI configuration than in the GI one, indicating that the large orbital magnetic moments remain in the NI setup. Figure 2(c) shows the integrated XMCD signals of the Fe *L*-edges for both NI and GI setups. A difference can be clearly observed in the residuals of the integrals for both L_3 and L_2 peaks. These integrated XMCD spectra indicate that the large orbital magnetic moments are enhanced in the NI geometry compared with those in GI one. This is reasonable for a Fe/MgO interface with a PMA related to the orbital magnetic moments. In addition, the magnetic field dependence of XMCD at L_3 peak from the NI geometry, shown in the inset of Fig. 2, reveals the large PMA of Fe.

Using the magneto-optical sum rules for the estimation of orbital and spin magnetic moments, we list the results for both the 300 and 450 °C annealing cases with the NI and GI geometries in Table I. The effective spin magnetic moments (m_{spin}) values were determined only from the GI geometry because the magic angle geometry of 57.3° from the surface normal can theoretically neglect the magnetic dipole terms.[24] For the application of the sum rules, we assumed the hole numbers of the Fe 3*d* states to be 3.4 as a standard value of Fe bulk.[25] For the 450 °C annealing case, the results listed in Table I show that the orbital magnetic moments with $m_{orb}{}^{\perp}$ of 0.30 and $m_{orb}{}^{\parallel}$ of 0.21 μ_B were calculated. In contrast, for the 300 °C annealing case, the difference in the orbital magnetic moments ($\Delta m_{orb} = m_{orb}{}^{\perp} - m_{orb}{}^{\parallel}$) is reduced compared to that in the case of 450 °C. Next, considering the Bruno relationship: $K \simeq (\xi/4)\ \alpha\ \Delta m_{orb}$, where ξ is the spin-orbit coupling constant, and α is the band-structure parameter, the PMA energies are proportional to Δm_{orb}. For the 450 °C case, we obtained $K = 130$ μeV/atom, which corresponds to a PMA value of 1.48 mJ/m^2, assuming a Fe lattice constant of 0.287 nm with a body-centered-cubic structure facing the MgO at the interface. For the 300 °C annealing case, the difference in orbital magnetic moments is smaller than that in the case of 450 °C annealing. In the former case, a K of 77 μeV/atom was estimated, which is smaller than that calculated in the latter case. These values are comparable to the results obtained by SQUID-VSM, shown in Fig. 1, although the magnetization measurements were performed at room temperature. It must be noted that magnetization measurements at low temperatures are difficult owing to the strong diamagnetic contribution from the large volume of the MgO substrates, which interrupts the intrinsic magnetic contribution from the thin Fe layers. Therefore, the element-specific XMCD measurements in the Fe *L*-edges constitute a unique technique for probing the magnetism of ultrathin Fe layers on MgO. The VSM results suggesting that the 450 °C annealing process enhances the PMA at the 0.7-nm-thick Fe/MgO interface are consistent with those obtained by XMCD and the subsequent analysis, which indicates that the contribution

TABLE I. Spin and orbital magnetic moments estimated from the XMCD sum rules for Fe at the Fe/MgO interface with annealing at 300 and 450 °C. The in-plane ($m_{orb}{}^{\parallel}$) and out-of-plane ($m_{orb}{}^{\perp}$) components are listed in units of μ_B. The PMA amplitudes obtained from XMCD in units of mJ/m^2 are also shown with those from SQUID-VSM.[8]

Annealing temperature	300 °C		450 °C	
	$m^{\perp}[\mu_B]$	$m^{\parallel}[\mu_B]$	$m^{\perp}[\mu_B]$	$m^{\parallel}[\mu_B]$
m_{spin} [μ_B]	…	2.07	…	2.08
m_{orb} [μ_B]	0.24	0.19	0.30	0.21
$K_i{}^{XMCD}$ (K^{XMCD})	0.86 mJ/m^2	(77 μeV/Fe)	1.48 mJ/m^2	(132 μeV/Fe)
$K_i{}^{VSM}$	1.19 mJ/m^2		2.01 mJ/m^2	

of the anisotropic orbital magnetic moments is essential for the appearance of PMA at the Fe/MgO interface.

Here, we discuss the origin of the PMA at the interface of Fe/MgO. Since the excitation processes in XMCD are regarded to be the atomic excitations from the core to unoccupied states, one can estimate the magnetic anisotropy energy per atom through the Bruno's relation by using the element-specific orbital magnetic moments. Since the diamagnetic and shape-anisotropic components of the magnetic anisotropy energy do not depend on the anisotropic orbital magnetic moments, the interface PMA values in units of J/m^2 were directly estimated. The contribution of K_{eff} should be calculated by using the diamagnetic components and the ultrathin Fe layer thickness, which is the same process as the estimation of PMA values using DFT calculations.

Next, we discuss the PMA values obtained by XMCD and the comparison with other experimental and theoretical works reported in the literature. The DFT calculations determine a magneto-crystalline anisotropy energy of 0.2 meV/atom in a free-standing Fe with 1 ML in thickness, a value of 0.9 meV/atom at the Fe (1 ML)/MgO interface, and 1.5 meV/atom at the MgO/Fe (1 ML)/MgO sandwiched structures.[16] These results suggest that the PMA of the Fe/MgO interface is enhanced with a double-facing interface. Considering that the obtained PMA value of 0.132 meV/(Fe atom) through the XMCD measurement for Fe (5 MLs)/MgO structure after annealing at 450 °C, the result is somewhat smaller than the estimated value from the DFT calculation (0.2 meV/Fe atom).[16] It is noted that the value for $m_{\mathrm{orb}}{}^{\parallel}$ can be underestimated, because the angle for the X-ray incident in the NI configuration was not exactly parallel to the film plane, i.e., 60°.Therefore, the PMA values can be estimated to be small relative to those from DFT calculations. Nevertheless, the estimated value of PMA through angular dependent XMCD for Fe (5 MLs)/MgO (001) structure, without an applied external electric field, was turned out to be comparable to that from the literature on the modulation of PMA by an electric field.[12–17]

Considering the above results, the origin of PMA at the Fe/MgO interface can be described by the anisotropic orbital magnetic moments induced by the spin-orbit interaction at the interface. The anisotropic orbital magnetic moments, resulting from the modulation of the occupancies of the Fe 3*d* states at the interface, were obtained through the sum-rule analysis of the XMCD spectra. Figure 3 displays the schematic energy diagram of the Fe 3*d* states at the Fe/MgO interface. First, the Fe 3*d* levels split into e_{g} and $t_{2\mathrm{g}}$ states due to the crystal field. At the surface or the interface accompanied with the symmetry breaking, the degenerated e_{g} states of the $d_{x^2-y^2}$ and d_{z^2} orbitals split further because of the surface field and the hybridization with the O $2p_z$ orbital. The spin-orbit interaction induces further splitting depending on the direction of the $\boldsymbol{H}_{\mathrm{ext}}$ and the magnetic quantum number m (0, ±1, and ±2). The d_{yz} and d_{zx} orbitals corresponding to $m=1$ consist of the complex orbitals denoted as the d_{yz+izx} and d_{yz-izx} states.[18] The anisotropy of charge occupancy between these complex states results in the anisotropic orbital magnetic moments. As was also indicated in the DFT calculations, the Fe $3d_{z^2}$ states are pushed up above the Fermi level through the hybridization with the O $2p_z$ orbital and the charge occupancies are modulated.[7] In addition, only when the $\boldsymbol{H}_{\mathrm{ext}}$ perpendicular to the film plane, the modulation in the electron occupancies results in the enhanced $m_{\mathrm{orb}}{}^{\perp}$. Therefore, due to the enhancement of $m_{\mathrm{orb}}{}^{\perp}$ resulted from the spin orbit interaction and the hybridization between Fe $3d_{z^2}$ and O $2p_z$ orbitals, the large PMA can be expected for the Fe/MgO interface. It is well coincided with our XMCD results for the NI configuration, which showed enhanced $m_{\mathrm{orb}}{}^{\perp}$.

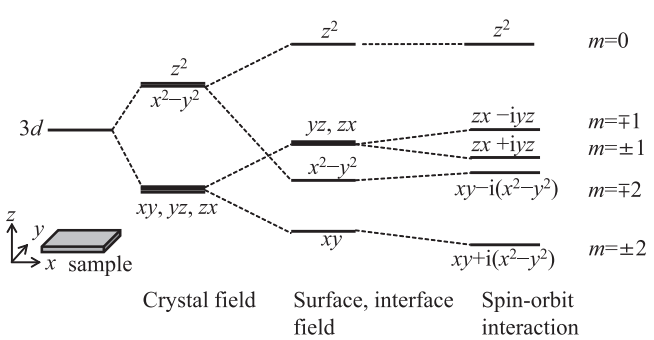

FIG. 3. Schematic diagram of the Fe 3*d* states with the crystal field, surface field, and spin-orbit interaction.

In conclusion, we have studied the interface PMA in ultrathin Fe/MgO (001) using angular-dependent XMCD. We found that the anisotropic orbital magnetic moments determined from the analysis of XMCD contribute to the large PMA energy, whose values depend on the annealing temperature. The large PMA energies deduced from the magnetization measurements are almost consistent with those estimated from the anisotropic orbital magnetic moments through the spin-orbit interaction. The enhancement of orbital magnetic moments can be explained by the hybridization between the Fe $3d_{z^2}$ and O $2p_z$ states at the Fe/MgO interface.

This work has been performed under the approval of the UVSOR facility programs at the Institute of Molecular Science, Japan. This work was partly supported by Nanotechnology Platform Program (Molecule and Material Synthesis) and a Grant-in-Aid for Young Scientists (A) (Grant No. 24686007) of Japan Society for the Promotion of Science (JSPS).

[1]S. Yuasa, T. Nagahama, A. Fukushima, Y. Suzuki, and K. Ando, Nat. Mater. **3**, 868 (2004).
[2]S. Ikeda, K. Miura, H. Yamamoto, K. Mizunuma, H. D. Gan, M. Endo, S. Kanai, J. Hayakawa, F. Matsukura, and H. Ohno, Nat. Mater. **9**, 721 (2010).
[3]K. Spörl and D. Weller, J. Magn. Magn. Mater. **93**, 379 (1991).
[4]A. Hallal, H. X. Yang, B. Dieny, and M. Chshiev, Phys. Rev. B **88**, 184423 (2013).
[5]S.-C. Lee, K.-S. Kim, S.-H. Lee, U.-H. Pi, K. Kim, Y. Jang, and U. Chung, J. Appl. Phys. **113**, 023914 (2013).
[6]J. Okabayashi, H. Sukegawa, Z. C. Wen, K. Inomata, and S. Mitani, Appl. Phys. Lett. **103**, 102402 (2013).
[7]H. X. Yang, M. Chshiev, B. Dieny, J. H. Lee, A. Manchon, and K. H. Shin, Phys. Rev. B **84**, 054401 (2011).
[8]J. W. Koo, S. Mitani, T. T. Sasaki, H. Sukegawa, Z. C. Wen, T. Ohkubo, T. Niizeki, K. Inomata, and K. Hono, Appl. Phys. Lett. **103**, 192401 (2013).
[9]C.-H. Lambert, A. Rajanikanth, T. Hauet, S. Mangin, E. E. Fullerton, and S. Andrieu, Appl. Phys. Lett. **102**, 122410 (2013).
[10]A. Koziol-Rachwal, W. Skowronski, T. Slezak, D. Wilgocka-Slezak, J. Przewoznik, T. Stobiecki, Q. H. Qin, S. van Dijken, and J. Korecki, J. Appl. Phys. **114**, 224307 (2013).
[11]P. Bruno, Phys. Rev. B **39**, R865 (1989).

[12]D.-S. Wang, R. Wu, and A. J. Freeman, Phys. Rev. B **47**, 14932 (1993).
[13]M. K. Niranjan, C.-G. Duan, S. S. Jaswal, and E. Y. Tsymbal, Appl. Phys. Lett. **96**, 222504 (2010).
[14]K. Nakamura, R. Shimabukuro, Y. Fujiwara, T. Akiyama, T. Ito, and A. J. Freeman, Phys. Rev. Lett. **102**, 187201 (2009).
[15]K. Nakamura, T. Akiyama, T. Ito, M. Weinert, and A. J. Freeman, Phys. Rev. B **81**, 220409(R) (2010).
[16]R. Shimabukuro, K. Nakamura, T. Akiyama, and T. Ito, Phys. E **42**, 1014 (2010).
[17]F. Bonell, Y. T. Takahashi, D. D. Lam, S. Yoshida, Y. Shiota, S. Miwa, T. Nakamura, and Y. Suzuki, Appl. Phys. Lett. **102**, 152401 (2013).
[18]J. Stohr, J. Magn. Magn. Mater. **200**, 470 (1999).
[19]B. T. Thole, P. Carra, F. Sette, and G. van der Laan, Phys. Rev. Lett. **68**, 1943 (1992).
[20]P. Carra, B. T. Thole, M. Altarelli, and X. Wang, Phys. Rev. Lett. **70**, 694 (1993).
[21]S. Yang, H.-K. Park, J.-S. Kim, J.-Y. Kim, and B.-G. Park, J. Appl. Phys. **110**, 093920 (2011).
[22]M. Sicot, S. Andrieu, F. Bertran, and F. Fortuna, Phys. Rev. B **72**, 144414 (2005).
[23]T. Yokoyama, T. Nakagawa, and Y. Takagi, Int. Rev. Phys. Chem. **27**, 449 (2008).
[24]T. Koide, H. Miyauchi, J. Okamoto, T. Shidara, A. Fujimori, H. Fukutani, K. Amemiya, H. Takeshita, S. Yuasa, T. Katayama, and Y. Suzuki, Phys. Rev. Lett. **87**, 257201 (2001).
[25]C. T. Chen, Y. U. Idzerda, H.-J. Lin, N. V. Smith, G. Meigs, E. Chaban, G. H. Ho, E. Pellegrin, and F. Sette, Phys. Rev. Lett. **75**, 152 (1995).